

Comparison of Properties of Carbon Particles Formed by Pyrolysis of C_3O_2 and C_2H_2 behind Shock Waves

H. Gg. Wagner*, A. V. Emelianov**, A. V. Eremin**, and H. Jander*

* *Institut für Physikalische Chemie, Georg-August Universität, Göttingen, 37077 Germany*

** *Institute for High Energy Density Associated Institute for High Temperatures, Russian Academy of Sciences, Moscow, 127412 Russia*

Received March 25, 2002

Abstract—Various carbon particles formed by the pyrolysis of C_3O_2 and C_2H_2 behind shock waves in the temperature range 1200–3800 K are studied. The formation of the condensed carbon particles is observed directly by the multichannel detection of the time profiles of the extinction of the medium in the UV, visible, and near-IR spectral regions. The samples of carbon material deposited on the walls of a shock tube after an experiment are analyzed using transmission electron microscopy with different resolutions and electron microdiffraction. Particles formed from C_3O_2 and C_2H_2 at 1500–2000 K are 10–30 nm in size and look like usual soot. The absence of molecular hydrogen in C_3O_2 only results in faster formation and graphitization. At 2100–2600 K, the formation of particles is retarded, and the yield of the carbon particles decreases for both substances. After experiments on pyrolysis of C_3O_2 at these temperatures, giant spherical particles up to 700 nm in size are found on the walls of the shock tube. Carbon particles formed at the highest temperatures (2700–3200 K) in C_3O_2 pyrolysis have the high degree of crystallinity of particles.

INTRODUCTION

The formation of carbon particles in high-temperature gas reactions is a complicated physicochemical process. Growing particles have different sizes and structures, and the kinetics of their formation is rather complicated. These phenomena have been reported in many papers, most of which are devoted to the formation of soot particles in flames and in hydrocarbon pyrolysis. Various hypotheses, which are under constant discussion and development, were proposed for the interpretation of the specific features of the processes [1, 2].

The possibility of obtaining carbon nanoparticles with certain properties (fullerenes, nanotubes, carbynes, and ultradispersed diamonds) in high-temperature gas reactions is of special interest. These processes remain unstudied, and further experimental studies are needed to obtain a general concept of this diverse phenomenon.

Data of experiments on the pyrolysis of hydrocarbons in shock tubes make a substantial contribution to the understanding of the kinetics of formation of carbon particles [3, 4]. Pyrolysis of different carbon-containing molecules has recently been studied in the absence of hydrogen (CCl_4 , C_3O_2), and the condensation of carbon vapor to small particles was simulated [5–9]. In these experiments, the authors observed a substantial yield of the particles in a wide temperature range from 1200 to 3500 K. The induction period for the formation of carbon particles from CCl_4 and C_3O_2 was shorter and the rate constant of their growth was higher than those

for the particles formed from hydrocarbons. Furthermore, the optical properties of these particles measured behind the shock wave differ substantially from those of usual soot [7]. Finally, the samples taken from the walls of a shock tube after experiment sometimes were white or light yellow [5, 6] and sometimes looked like solidified droplets [8].

These results raised the questions, what is the difference between the mechanism of formation of particles during the pyrolysis of carbon-containing hydrogen-free molecules and the mechanism of soot formation from hydrocarbons? Can this difference result in different structures of the carbon particles?

Based on microdiffraction analysis, Frenklach [5] explained the white color of particles obtained during CCl_4 pyrolysis by the presence of carbyne crystals. On the other hand, electron microscopic analysis of the particles obtained by C_3O_2 pyrolysis [8] showed that they had a layered crystalline structure with a distance between layers of ~0.25–0.35 nm, indicating that they belong to graphite.

The main purpose of this work was to examine the spectroscopic and structural properties of carbon nanoparticles formed by C_3O_2 and C_2H_2 pyrolysis in a wide temperature range.

EXPERIMENTAL

Experiments were carried out in a standard shock tube with an inner diameter of 70 mm and a low-pressure chamber 4.5 m long. The formation of condensed

carbon particles was monitored by the multichannel detection of the time profiles of the optical properties of the medium in the UV, visible, and IR spectral regions. With this purpose, the attenuation of the transmitted radiation (extinction) and radiation of the medium (emission) were measured in each experiment at 400, 473, 516, and 633 nm and at 1.31 μm . The latter was carried out by the probing radiation modulation method with a frequency of 300 kHz. The detection of emission signals made it possible to take into account the contribution of the intrinsic radiation of the medium to the measured extinction level. A high-pressure discharge xenon lamp and He–Ne (633 nm) and IR-diode (1.31 μm) lasers served as radiation sources. Interference filters, photoamplifiers, IR detectors, digital oscillographs, and computers were used for the detection of signals.

Mixtures consisting of 0.2–2.0% C_3O_2 or C_2H_2 diluted with argon were subjected to pyrolysis. Measurements were carried out behind reflected shock waves in a wide temperature range (1200–3800 K) at pressures from 10 to 60 atm. The parameters of gases behind shock waves were calculated from the rate of the incident shock wave taking into account the real thermodynamic parameters of the mixtures used. High-temperature (2500–3800 K) experiments were carried out at different distances between the measured cross-section and the edge of the shock tube, which were varied from 4 to 138 mm. The residence time of gas behind the incident shock wave (first heating) before the arrival of the reflected shock wave (secondary heating) varied from 10–15 μs to 1000–1500 μs .

After each experiment, the samples of particles collected from the walls of the shock tube were analyzed using a transmission electron microscope (TEM) with low and high resolutions and using electron microdiffraction measurements using a Philips ELMI 420 instrument. For TEM measurements, the samples were placed on a copper grid covered by a carbon film 3 mm in diameter with 400 meshes. This type of grid allows one to observe particles on the edges of the free space of the lattice.

The particles were analyzed as follows.

1. Measurements by low-resolution TEM (LRTEM) with an amplification of $m < 100000$, which allow one to see the shape of particles and estimate their sizes. These measurements give the particle size distribution, the average diameter (d), and the root-mean-square deviation (σ).

2. Measurements using high-resolution TEM (HRTEM) with an amplification of $200000 \leq m \leq 500000$ make it possible to observe the fine structure of a specific particle, the region and state of crystallization, and the planes of the layers and distances between them.

3. Electron microdiffraction measurements (EMD) confirm the crystal structure when the Bragg conditions for interference are fulfilled.

RESULTS

Time and Spectral Extinction Profiles¹

The time profiles of the extinction measured in the pyrolysis of all molecules under study were processed using the Lambert–Beer law by the equation determining the optical density (D) at a certain wavelength λ as a function of time and weakening of the probe signal:

$$D(t) = -\frac{\ln(I_\lambda(t)/I_\lambda(0))}{[C]} \quad (1)$$

Here $I_\lambda(t)$ and $I_\lambda(0)$ are the intensities of the transmitted light experimentally measured at the time moments t and 0, respectively. For the convenience of comparing data from different experiments, the optical density in formula (1) was attributed to the maximal achieved concentration of the carbon atoms $[C]$.

A typical example of such experiments is shown in Fig. 1. It is clearly seen that an increase in the extinction in the UV spectral region is faster than those in the visible and, especially, IR regions. That is, the particle growth is accompanied by the extension of the extinction spectrum from the short-wave to the long-wave region. This phenomenon is observed for the particles formed by C_2H_2 and C_3O_2 pyrolysis in the 1500–2100 K temperature range. Thus, the primarily particles are “transparent” in the visible and IR spectral regions and absorb only in the UV region. At the end of the experiment, the particles become completely “black.”

At temperatures higher than 2000–2200 K, the situation changes. The rate of extinction growth in the UV region still increases with temperature. However, the extinction in the visible and IR regions increases more slowly, and the resulting spectrum is different. The extinction spectra of the particles obtained from C_3O_2 measured at different times and temperatures are shown in Fig. 2. It is seen that the resulting spectrum of the carbon particles, which are formed very rapidly (within $<15 \mu\text{s}$) at $T = 2214 \text{ K}$ (curve 4) differs from the spectrum of particles formed at $T = 1646 \text{ K}$ for $>300 \mu\text{s}$ (curve 3). The maxima in the spectra observed at $\lambda = 516 \text{ nm}$ in all plots are explainable by the Swan bands for the C_2 radicals.

Final Extinction Level

The next step in data processing was the analysis of the temperature plot of the final extinction level. The

plots of the final extinction ($D_{\text{max}} = \frac{\ln I_{\text{max}}(t)/I(0)}{[C]}$)

vs. T at $\lambda = 633 \text{ nm}$ and $\lambda = 1.31 \mu\text{m}$ for C_2H_2 and C_3O_2 pyrolysis are shown in Fig. 3. It is seen that for C_3O_2 the plot represents the curve with two maxima whose positions differ at different wavelengths. For the pyrolysis

¹ Henceforth, extinction implies the attenuation of the radiation transmitted through the medium, which is the sum of two processes: intrinsic absorption and scattering.

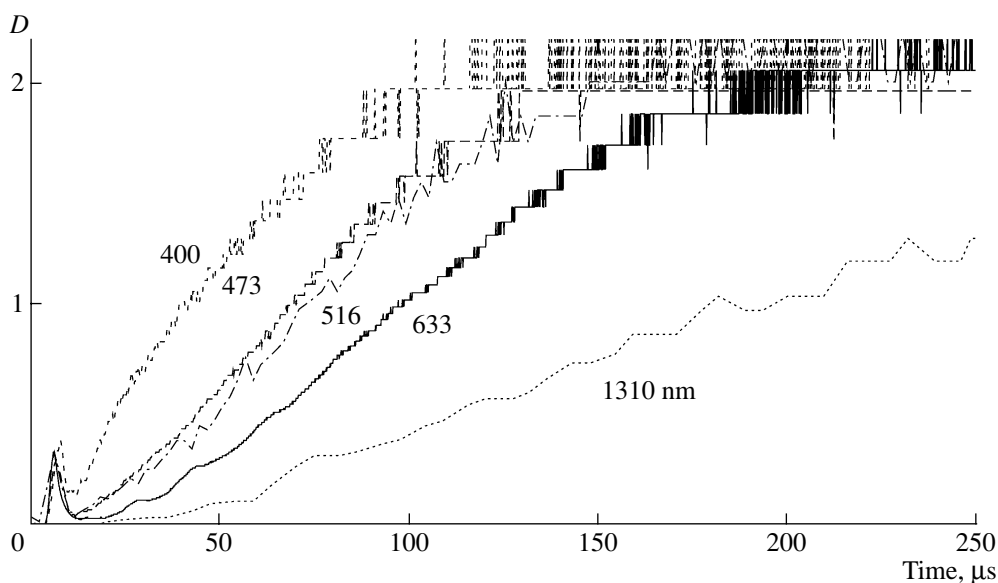


Fig. 1. Time profiles of the optical densities measured simultaneously at different wavelengths (indicated in the curves) from the UV to IR spectral regions. Experimental conditions: 1% C₃O₂ in Ar, $T = 1548$ K $P = 28$ atm. Initial peaks: schlieren signals of the front of the reflected shock wave.

of a 1% C₂H₂-Ar mixture (Fig. 3b), the second extinction maximum at high temperatures was not observed. However, the second bell-shaped maximum was observed in preliminary experiments [10] for a 2% C₂H₂-Ar mixture. It is noteworthy that the extinction decreases at temperatures higher than 2100 K for both substances (and in other systems) at all wavelengths.

Kinetics of the Optical Density Increase

Figure 4 represents the Arrhenius plots of the rate constants of the optical density increase k_λ calculated under the assumption that the first-order kinetic equation is fulfilled [8]:

$$\frac{dD(t)}{dt} = k_\lambda(D_{\max} - D(t)). \quad (2)$$

For both mixtures the plots $\ln k_\lambda = f(1/T)$ at $\lambda = 633$ nm and 1.31 μm (curves 2 and 3) have a break in the 1900–2200 K temperature range. At a higher temperature, the optical density increase at these wavelengths retards with temperature. At the same time, the rate constant of optical density increase measured at $\lambda = 400$ nm (curve 1) continues to rise with temperature.

Analysis of Particles Using TEM and EMD Methods

The solid carbon materials, which formed by C₃O₂ pyrolysis at 1650–3000 K and deposited on the walls of the shock tube, were studied with an electron microscope. The materials were predominantly black but in some high-temperature ($T \geq 3000$ K) experiments the samples were dark brown.

Several different types of particles were observed at low resolution (LRTEM). Spherical particles agglomerated in chains or more compact structures with different sizes were the most typical. These particles were observed at all temperatures, and their average diameter d_g and the root-mean-square deviation σ_g were determined. The results are presented in Table 1. The average diameter of the particles differs at three different temperatures, and d_g at $T = 2214$ K is four- to fivefold

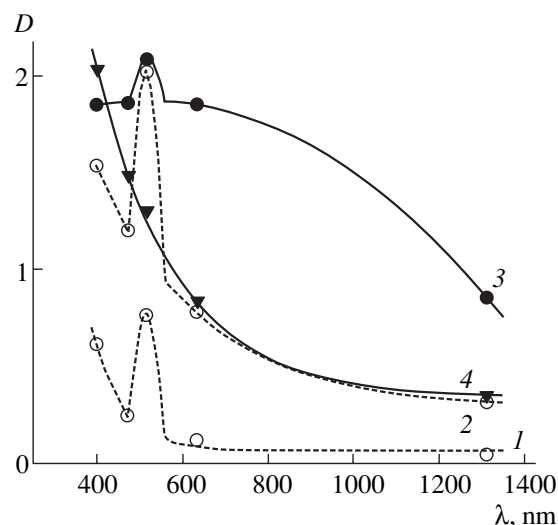


Fig. 2. Extinction spectra of the particles obtained by C₃O₂ pyrolysis at different times and temperatures. Dotted lines show the current spectra measured at $T = 1646$ K at the time moments $t = (1)$ 60 and (2) 150 μs . Solid lines show the spectra of the resulting particles measured at $T = (3)$ 1646 and (4) 2214 K in the last, stationary step of the process.

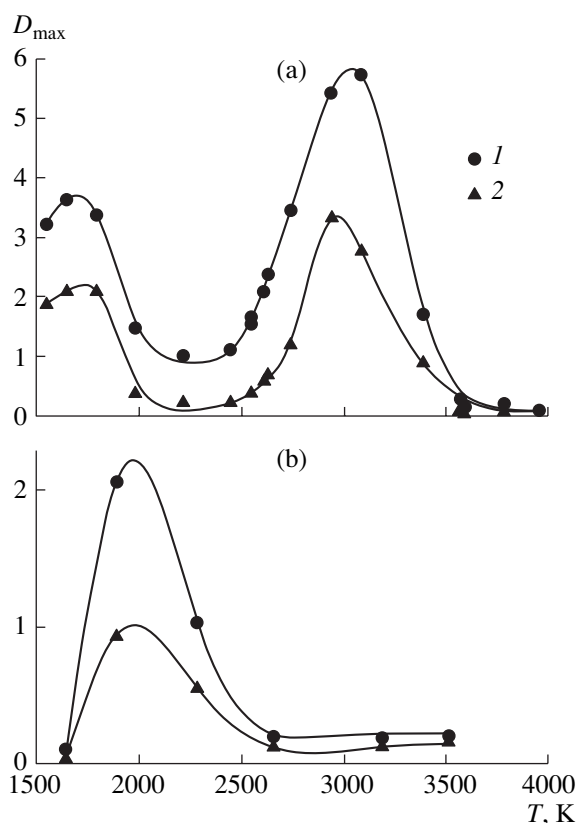


Fig. 3. Temperature plots of the maximal optical density (D_{\max}) at (1) 633 nm and (2) 1.31 μm observed for (a) 1% C_3O_2 -Ar and (b) 1% C_2H_2 -Ar mixtures. At $T > 2500$ K the measurements were carried out at the distance $L = 59$ mm from the edge of the shock tube.

greater than those at $T = 1646$ and 3002 K; that is, the temperature plot of d_g has a maximum in this temperature range. The same behavior of the particles can be observed by HRTEM analysis of the samples. The structures of the samples obtained at three different temperatures are shown in Fig. 5. The particles formed at 1646 K (Fig. 5a) have no crystalline structure and form chains from almost spherical primary particles. The samples have a developed surface and a multilevel structure of particular particles. This result reflects the amorphous nature of the particles, which is also confirmed by microdiffraction studies.

Particles of two radically different types are formed at $T = 2214$ K (Figs. 5b, 5c). Particles of one type (Fig. 5b) have pronounced spherical components whose size is much greater than the size of particles observed at $T = 1646$ K (see Table 1). The HRTEM observations show that these large particles have a developed multilayer surface and are similar to those formed at 1646 K. However, they contain some small regions of crystallization. The particles of the other type obtained at this temperature (Fig. 5c) are giant ($d \sim 700$ nm). They look like thin films where the crystallization threads pass through the whole region of par-

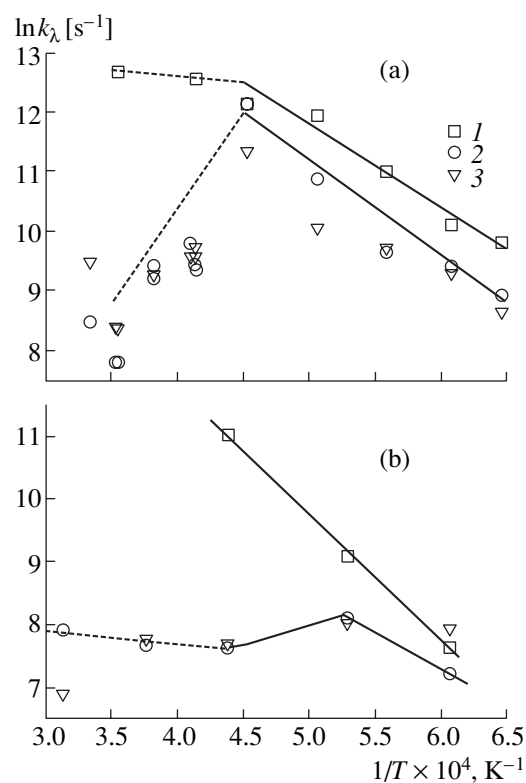


Fig. 4. Arrhenius plots of the rate constant of the optical density increase at (1) 400 nm, (2) 633 nm, and (3) 1.31 μm for (a) 1% C_3O_2 -Ar and (b) 1% C_2H_2 -Ar mixtures. The curves were drawn using the least-squares method.

ticles. The whole particle is surrounded by this crystalline structure consisting of four to six atomic layers. When the temperature of particle formation increases ($T > 2300$ K), these two different types are retained, and their regions of crystallization increase. The development of the regions of crystallization is shown in Fig. 5d. At $T = 3002$ K they look like developed crystalline structures with different lengths, which sometimes consist of two or three atomic layers.

Particles obtained at $T < 2000$ K are amorphous and cannot be studied by EMD. Among the particles formed at $T > 2000$ K, only carbon materials obtained by C_3O_2 pyrolysis were subjected to EMD analysis. For $T = 2214$ K, the diffraction pattern could only be obtained for the giant particles, whereas for $T = 3002$ K EMD measurements were possible for both types of particles, which is explained by the extended region of crystallization in the latter. The microdiffraction pattern is shown in Fig. 6 and demonstrates the structure of the pronounced rings corresponding to the interplanar distances d_{002} , d_{110} , and d_{100} . The results of EMD measurements are presented in Table 2 along with data for graphite [11], carbyne [12], and testing measurements of black carbon for comparison.

Thus, the properties of particles of two different types were studied: the optical properties of “young” particles during their formation and the size and structure of the samples deposited on the walls of the shock tube after cooling. The main problem was to combine the results obtained and to draw some conclusions about the formation of the particles in different substances and at different temperatures.

DISCUSSION

The specific features of formation and the properties of the carbon particles make it possible to divide the temperature range under study from 1200 to 3500 K into several subranges: 1500–2000, 2100–2600, 2700–3200, and >3200 K. Our experiments confirmed the presence of two maxima in the temperature plot of the extinction in the visible (633 nm) and IR (1310 nm) spectral regions for the particles obtained from C_3O_2 [8] (see Fig. 3a). Let us compare these curves with data from other measurements and attempt to obtain some idea of the real properties of particles.

The low-temperature range 1500–2000 K is the most studied. This is the range of the highest yield of soot in flames and in experiments on hydrocarbon pyrolysis in shock waves [3]. The results of this work also showed a substantial yield of particles in this range. The extinction maximum at different wavelengths was observed for the C_3O_2 mixture at $T \sim 1600$ –1700 K and for the C_2H_2 mixture at $T \sim 1800$ –1900 K. The temperature dependence of the rate constants of extinction (usually named the “rate constants of particle formation”) in the range 1500–2000 K are described by the Arrhenius law with the activation energy ~ 200 kJ/mol

Table 1. Average diameter of carbon particles (d_g) and the root-mean-square deviation (σ_g)*

T , K	d_g , nm	σ_g
1646	14.0	0.18
2214	65.0	0.30
3002	22.4	0.21

* A 1% C_3O_2 –Ar mixture.

for all wavelengths and all substances. Note that the $k_\lambda(T)$ plot measured for C_3O_2 at 400 nm in the 1500–2000 K range is very close to the rate constant of C_3O_2 decomposition [13]. This indicates the substantial role of the C_3 radicals, which exhibit an intense absorption band at $\lambda = 400$ nm under these conditions.

Particles obtained by C_3O_2 pyrolysis are similar in size and structure (TEM data) to the soot particles obtained from C_2H_2 and by the pyrolysis of other hydrocarbons (see Fig. 5). Nevertheless, the optical properties of the particles from C_3O_2 differ from the optical properties of soot formed from hydrocarbons. Dörge *et al.* [7] pointed to the fact that the molar absorption coefficients of these particles are two- to threefold higher than those for soot formed from hydrocarbons. To describe these particles, they proposed to use the refractive index $m = n - ik$ with the real part for soot $n = 1.57$ and the imaginary part for graphite $k = 1.4$. Our observations confirm this conclusion and show a significant deviation of the spectral extinction coefficient for the particles formed by C_3O_2 pyrolysis from that for usual soot particles formed from C_2H_2 .

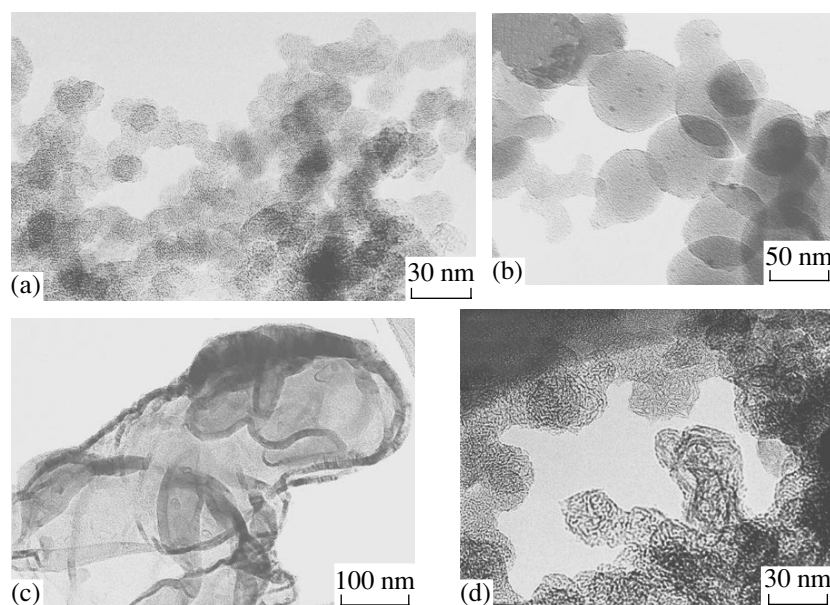


Fig. 5. High-resolution electron microscopic patterns of the carbon particles formed by C_3O_2 pyrolysis at temperatures (a) 1646, (b, c) 2214, and (d) 3002 K.

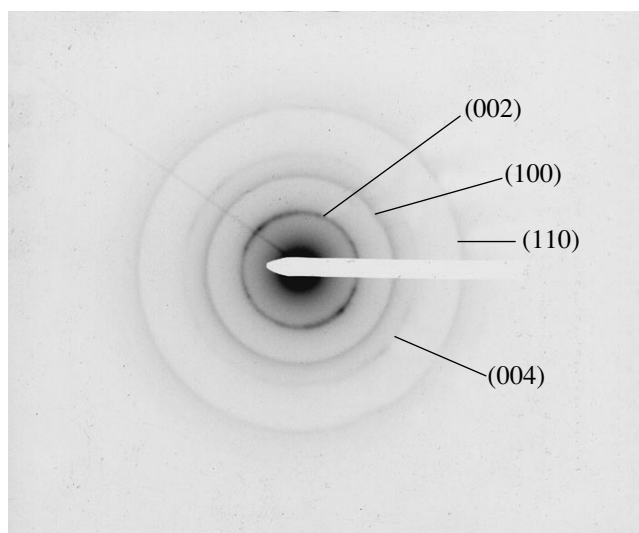


Fig. 6. Microdiffraction pattern of the carbon particles obtained by C_3O_2 pyrolysis at $T = 2214$ K. The lines denoted by figures in parentheses characterize the interplanar distances (d_{hkl}) for the particles under study.

The temperature plots of the optical density (ER_{\max}) at $\lambda_1 = 1310$ nm and $\lambda_2 = 633$ nm are shown in Fig. 7.

$$ER_{\max} \equiv \frac{\ln(I_{\max,1}(t)/I(0)_1)}{\ln(I_{\max,2}(t)/I(0)_2)} \quad (3)$$

$$\approx \frac{\sigma_{\text{ext}}(\lambda_1)}{\sigma_{\text{ext}}(\lambda_2)} = \frac{\sigma_{\text{scat}}(\lambda_1) + \sigma_{\text{abs}}(\lambda_1)}{\sigma_{\text{scat}}(\lambda_2) + \sigma_{\text{abs}}(\lambda_2)},$$

where σ_{ext} , σ_{abs} , and σ_{scat} are the cross-sections of extinction, absorption, and scattering for the finally formed particles at both wavelengths. One can see a gradual increase in ER_{\max} with temperature for the soot particles from C_2H_2 and the very specific behavior of ER_{\max} for the particles formed by C_3O_2 pyrolysis. In the 1500–2000 K temperature range, the data for soot obtained from C_2H_2 agree with $\lambda_2/\lambda_1 = 0.48$, which follows from the Mie theory describing the light absorption and scattering by small particles [14]. At the same

time, the ER_{\max} values for the particles from C_3O_2 decrease sharply, most likely indicating a decrease in the average size of the particle. This result agrees with the decrease in the absolute extinction at all wavelengths in this temperature range observed for the particles for C_3O_2 pyrolysis (see Fig. 3 and [7, 8]).

The next temperature range from 2100 to 2600 K seems to be the most special. The optical density of particles formed behind the reflected shock wave begins to decrease for C_3O_2 at $T \sim 1800$ K and for C_2H_2 at $T \sim 2000$ K (see Fig. 3). As mentioned above, these data can indicate a decrease in the size of particles formed at these temperatures. This logical conclusion agrees with the results on light scattering [4], the measurements of the particle size by laser-induced incandescence [15], and the numerical simulation of the formation of the particles by C_3O_2 pyrolysis [16].

One more specific feature of particle formation observed at these temperatures is known as a break in the Arrhenius plot of the rate constant of the extinction growth. In this work, this break is observed for the pyrolysis of C_2H_2 at $T \sim 1900$ K, and for C_3O_2 it is observed in the interval 2000–2100 K in the visible and IR spectral regions, which is in good accord with previous data [3, 6, 9].

The particles deposited on the walls of the shock tube after experiments on C_3O_2 pyrolysis at these temperatures substantially differ from usual soot particles. They are mainly black or dark brown. After some experiments, the spots of a bright black substance, which look like a solidified liquid, were found on the walls of the shock tube. Contrary to *in situ* measurements, TEM analysis of these samples shows unusually large, giant particles resembling film balls with a diameter of up to 700 nm.

In order to eliminate the contradiction between the small size of the particles observed behind the shock wave and the giant solidified droplets on the walls after experiment, it should be taken into account that the rate of formation of particles sharply decreases in this temperature range. Therefore, particles observed behind the shock wave for an accessible time of ~ 1 –1.5 ms are

Table 2. Interplanar distances (d_{hkl}) for different carbon materials

Substance	T , K	d_{002} , Å	d_{100} , Å	d_{110} , Å	d_{100}/d_{110}
Graphite [11]	300	3.3756	2.1386	1.234	1.733
Carbyne [12]	300	2.204	4.408	2.545	1.732
Black carbon (testing substance)	300	3.42	2.09	1.21	1.73
C_3O_2	2214	3.40	2.07	1.20	1.73
$C_3O_2^*$ (1)	3002	2.96	2.03	1.19	1.71
$C_3O_2^*$ (2)	3002	3.27	1.99	1.17	1.70

* (1) Results for spherical particles and (2) results for giant particles.

probably far from being in the thermodynamic equilibrium. These young particles most likely represent linear carbon polymers (carbynes), which could later form “liquid clusters and droplets” [17] and are agglomerated during cooling to form giant “consolidated droplets” or “spherules” [18]. It should be kept in mind that the microdiffraction analysis of giant droplets revealed no carbyne crystals but indicated their graphite structure. This fact can be explained by the strong dependence of the stability of carbyne on the rate of its cooling [17]. Evidently, in experiments in the shock tube the cooling rate is not too high and cooling occurs only in rarefied waves and during diffusion in the boundary layer.

The next interesting temperature range is 2700–3200 K. In this range, the yield of particles was observed for C_3O_2 pyrolysis only behind the reflected shock wave (“two-step heating”). In fact, direct heating (in the incident wave) did not result in a noticeable formation of particles. This fact was attributed in [8, 19] to the strong overexcitation of primary carbon clusters (C_2 radicals) at these temperatures, which could retard the further growth of the clusters. Two-step heating helps to surmount this phenomenon due to the efficient formation of small clusters behind the incident wave at temperatures of 1400–1600 K without overexcitation of the C_2 radicals. Thus, the further growth of the particles behind the reflected shock wave uses these nuclei.

The optical density at different wavelengths and the average particle size measured by TEM in this temperature range are again similar to those observed at 1500–2000 K; that is, in the region of the first maximum in the temperature plot. A significant difference and strong crystallization of the samples is shown by microdiffraction analysis only. The interplanar distances of these crystals also lie in the interval inherent in graphite. Nevertheless, d_{002} and d_{100} decrease insignificantly (see Table 2). Due to the strong (and probably, fast) crystallization at high temperatures (2700–3200 K), the observed extinctions and the resulting size of the particles coincide with the corresponding values for the particles formed at low temperatures of 1500–2000 K.

The temperature range $T > 3200$ K is characterized by a decrease in the yield of particles during C_3O_2 pyrolysis. The temperature increase most likely results in an increase in the rate of cluster decomposition. At $T \sim 3500$ – 3800 K, the decomposition rates exceed the rates of cluster growth [8], and no particles are formed.

CONCLUSIONS

A variety of the carbon particles formed by the pyrolysis of C_3O_2 and C_2H_2 behind the shock waves were studied in a wide temperature range (1200–3800 K). A comparison of the properties of the extinction of the growing particles with the electron microscopic analysis data for the samples of particles deposited on the

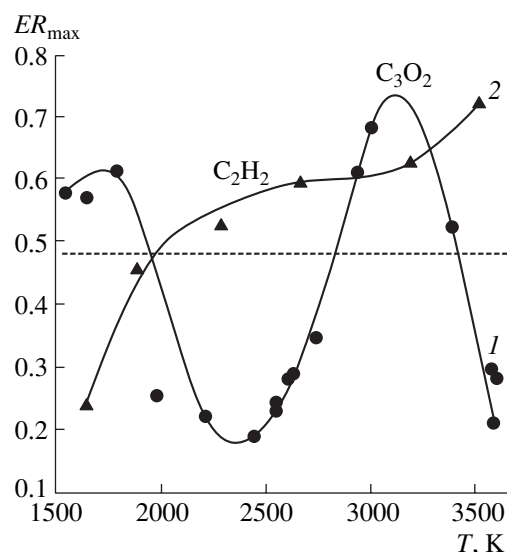


Fig. 7. Temperature plots of the ratios of extinctions measured (ER_{\max}) at $\lambda_1 = 1310$ nm and $\lambda_2 = 633$ nm for the pyrolysis of (1) C_3O_2 and (2) C_2H_2 at maximum times of 1–1.5 ms. Solid lines show the experimental data processed by the least-squares method. The dotted line shows the theoretical value $ER_{\text{theor}} \approx \lambda_2/\lambda_1 = 0.48$, which follows from the Mie theory for the absorption of small spherical particles ($d \ll \lambda$).

walls reveals the specific features of the formation of the carbon particles under different conditions.

1. Particles formed from C_3O_2 at standard temperatures of flames (1500–2000 K) look like usual soot from hydrocarbons (for example, C_2H_2): spheres 10–30 nm in size, and the absence of hydrogen results in the faster formation and graphitization of particles.

2. At 2100–2600 K, the rate of formation and the yields of particles decrease in all mixtures. After experiments on C_3O_2 pyrolysis, analysis of the EMD patterns of the samples of the particles taken from the walls of the shock tube showed that at these temperatures the giant film spherical particles with a size of up to 700 nm were observed. They could be formed due to the fast agglomeration of small “liquid clusters” during cooling of the particles on passing through rarefied waves.

3. The high degree of crystallinity of the resulting particles is a specific feature of the high-temperature (2700–3200 K) formation of the carbon particles by C_3O_2 pyrolysis. The acceleration of crystallization with temperature leads to a decrease in the agglomeration rate, and the size of the resulting particles again falls within the range 20–30 nm. The structure of crystals observed consists of hexagonal layers with a graphite-like spatial arrangement.

Special experiments with monitoring of the cooling rate of the particles are needed to obtain further information on the influence of the agglomeration process on the resulting structure of the particles.

ACKNOWLEDGMENTS

The authors thank Prof. E.I. Asinovskii for helpful discussions of the results. This work was supported by the Russian Foundation for Basic Research and DFG.

REFERENCES

1. Frenklach, M. and Wang, H., *Proc. Combust. Inst.*, 1991, vol. 23, p. 1559.
2. Krestinin, A.V., *Proc. Combust. Inst.*, 1998, vol. 27, p. 1557.
3. Bauerle, St., Karasevich, Yu., Slavov, St., *et al.*, *Proc. Combust. Inst.*, 1994, vol. 25, p. 627.
4. Kellerer, H., Koch, R., and Wittig, S., *Combust. Flame*, 2000, vol. 120, p. 188.
5. Frenklach, M., *Combust. Sci. Technol.*, 1990, vol. 74, p. 283.
6. Starikovskiy, A., Thienel, Th., Wagner, H.Gg., and Zaslanko, I., *Ber. Bunsen-Ges. Phys. Chem.*, 1998, vol. 102, p. 1815.
7. Dörge, K.J., Tanke, D., and Wagner, H.Gg., *Z. Phys. Chem.*, 1999, vol. 212, p. 219.
8. Deppe, J., Emelianov, A., Eremin, A., *et al.*, *Proc. Combust. Inst.*, 2000, vol. 28, p. 2515.
9. Wagner, H.Gg., Vlasov, P.A., Dörge, K.Yu., *et al.*, *Kinet. Katal.*, 2001, vol. 42, no. 5, p. 645.
10. Deppe, J., Emelianov, A.V., Eremin, A.V., *et al.*, *Z. Phys. Chem.*, 2000, vol. 214, p. 129.
11. JCPDS, International Center of Diffraction Data, 1997.
12. Borodina, T., Fortov, V., *et al.*, *J. Appl. Phys.*, 1996, vol. 80, p. 3757.
13. Friedrichs, G. and Wagner, H.Gg., *Z. Phys. Chem.*, 1998, vol. 203, p. 1.
14. Bohren, C. and Huffman, D., *Absorption and Scattering of Light by Small Particles*, New York: Wiley, 1983.
15. Eremin, A., Ziborov, V., Shumova, V., Starke, R., and Roth, P., *WIP Abstr. of XXIX Int. Symp. on Combustion*, Sapporo, 2002, p. 129.
16. Soika, J., Warnatz, J., Vlasov, P., and Zaslanko, I., *Combust. Sci. Technol.*, 2000, vol. 158, p. 439.
17. Asinovskii, E.I., Asinovskii, S.E., Borodina, T.I., *et al.*, *Karbin na fazovoi diagramme ugleroda* (Carbyne on the Phase Diagram of Carbon). Moscow: OIVT RAN, 2000, preprint no. 1-449, p. 13.
18. Wittaker, A. and Kintner, P., *Carbon*, 1985, vol. 23, p. 255.
19. Wagner, H.Gg., Deppe, J., Emelianov, A.V., Eremin, A.V., *et al.*, *Dokl. Ross. Akad. Nauk*, 2001, vol. 379, no. 1, p. 63.